JOURNAL OF MATERIALS SCIENCE **34** (1999) 675–681

Weibull master curves and fracture toughness testing

Part II *Evaluation of data of quasi-static three-point bend tests of tetragonal zirconia, zirconia/alumina and silicon nitride*

M. LAMBRIGGER
Centre de recherches en physique des plasmas, Technologie de la Fusion, EPFL, Im Struppen 12, CH-8048 Zürich, Switzerland

It has already been displayed that a variety of apparent fracture toughness master curves and Weibull master curves exist, which enables an extensive description of the fracture toughness of the investigated solids. Therefore, the concept of Weibull master curves has been generalized. In this paper, it is shown that characteristic magnitudes, derived from both experimental Weibull master curves and experimental apparent fracture toughness master curves, can be defined in a new way, by quantifying the amount of microcracking and crack-tip shielding that occurs when materials undergo stable crack growth prior to failure (when a sufficient external load is applied). Experimental data of three-point bend tests of ceria partially stabilized tetragonal zirconia, yttria partially stabilized zirconia/β-alumina-composite, and coarse-grained β-silicon nitride gathered at room temperature have been evaluated. The Weibull master curves, which are obtained by scaling the cumulative failure distribution functions with the corresponding mean-values, have been found to be most appropriate for investigating the fracture toughness by quasistatic uniaxial tensile or bend tests.

List of Symbols

c	Constant
σ	Applied failure stress
$P(\sigma)$	Three-parameter, cumulative Weibull failure probability distribution function
σ_0	Normalizing factor in dimensions of stress
σ_τ	Threshold stress, below which no failure occurs
σ_{in}	Failure stress at the inflexion point $P(\sigma)$
$\overline{\sigma}$	Mean failure stress
m	Weibull modulus
z	Distinct value of the cumulative failure probability distribution function
σ_z	Failure stress corresponding to the cumulative failure probability z
K_I	Failure stress intensity
$P(K_I)$	Cumulative failure probability distribution function in terms of K_I
$K_{\min}$	Threshold stress intensity, below which no failure occurs
K_{Iin}	Failure stress intensity at the inflexion point of $P(K_I)$
$\overline{K_I}$	Mean failure stress intensity
K_{Iz}	Failure stress intensity corresponding to the cumulative failure probability z

$I(x, m)$, $K(y, m)$ and $M[e(z), m]$:
Three different types of Weibull master curves

$I\exp(x, m)$, $K\exp(y, m)$ and $M\exp[e(z), m]$:
Three different types of experimental Weibull master curves

$N(a)$, $T(b)$ and $L[d(z)]$:
Three different types of master curves for brittle cleavage fracture toughness testing, i.e., three different types of theoretical, apparent fracture toughness master curves

$N\exp(a)$, $T\exp(b)$ and $L\exp[d(z)]$:
Three different types of experimental, apparent fracture toughness master curves

x, y and $e(z)$:
Different types of scaled failure stresses

a, b and $d(z)$:
Different types of scaled failure stress intensities

x_{cr}, y_{cr}, $e_{cr}(z)$, a_{cr}, b_{cr} and $d_{cr}(z)$:
Values of the cross-over points formed by the corresponding experimental and theoretical master curves

$H(x)$:
Step function being equal to zero for $x < 1$ and equal to one for $x \geq 1$

$Fih1$, $Fih2$, $F\exp1$, $F\exp2$ and χ:
Former deviation parameters derived from the Weibull master curves $I(x, m)$ and $I\exp(x, m)$ as well as the step function $H(x)$

$H[e(z)]$:
Step function being equal to zero for $e(z) < e_{cr}(z)$ and equal to one for $e(z) \geq e_{cr}(z)$

$FiM1[e(z)]$, $FiM2[e(z)]$, $F\exp1M[e(z)]$, $F\exp2M[e(z)]$, χ_M, χ_I and χ_k:
New deviation parameters derived from the Weibull master curves $M[e(z)]$ and $M\exp[e(z)]$ as well as the step function $H[e(z)]$

$C_{1\infty}$, $C_{2\infty}$, $C1\exp$, $C2\exp$ and χ_B:
Deviation parameters derived from master curves for brittle cleavage fracture toughness testing $L[d(z)]$ and experimental, apparent fracture toughness master curves $L\exp[d(z)]$

1. Introduction

In part 1 of this series of papers [1], the derivation and construction of all types of Weibull master curves $I(x, m)$, $K(y, m)$ and $M[e(z), m]$ have been described, as well as theoretical, apparent fracture toughness master curves $N(a)$, $T(b)$ and $L[d(z)]$. Moreover, the construction of experimental master curves has been shown in detail. Finally, the mathematical link between the quasi-static Weibull theory for uniaxial tensile and bend tests and the quasi-static Wallin theory for brittle cleavage fracture toughness testing has also been revealed.

In this paper, deviation parameters will be defined for experimental Weibull master curves and apparent fracture toughness master curves, which quantify the capacity of the investigated materials to undergo stable crack growth prior to failure. These deviation parameters will subsequently be determined and discussed for ceria partially stabilized tetragonal zirconia, yttria partially stabilized zirconia/β-alumina-composite, and coarse-grained β-silicon nitride by evaluating experimental data of quasi-static three-point bend tests performed at room temperature.

Lambrigger [2] has already shown that experimental Weibull master curves of materials undergoing an amount of stable crack growth prior to failure enable the characterization of the toughening mechanisms operating in the investigated materials. Furthermore, it has been shown that an experimental Weibull master curve $I\exp(x, m)$ of 8 wt % Y-PSZ/20 vol % β-alumina composites can be constructed in the case of materials undergoing stable crack growth prior to failure by simply calculating the Weibull modulus m from the upper failure stress range σ_i of experimental, cumulative failure stress probability distribution $P(\sigma_i)$ having been treated extensively in part 1 of this series of papers [1]. In order to evaluate experimental failure data (σ_i, $P(\sigma_i)$), a step function $H(x)$ equal to zero for scaled failure stresses $x < 1$ and equal to one for $x \geq 1$, as well as a quotient χ characteristic for the investigated material, have been defined by Lambrigger [2]. $H(x)$ represents a material undergoing 0% unstable crack extension. χ has thus been given by

$$\chi = \left(\frac{Fih1}{Fih2}\right) : \left(\frac{F\exp1}{F\exp2}\right) \tag{1}$$

where $Fih1$ and $Fih2$ denote the two areas formed between $H(x)$ and $I(x, m)$ in the range $0 \leq x \leq 1$. $F\exp1$ and $F\exp2$, however, represent the two areas formed between $I\exp(x, m)$ and $I(x, m)$ in the same x-range. The areas $Fih1$ and $F\exp1$ have been defined as being located below the cross-over x_{cr} of the respective bordering curves, whereas $Fih2$ and $F\exp2$ are located above x_{cr}. The quotient χ was assumed, in a first approach, as a specimen-size-independent, material-specific magnitude characterizing the toughening mechanisms operating in the investigated materials. Unfortunately, χ is a function of the material-specific Weibull modulus m [2], thus complicating quantitative comparisons between different types of materials, if the shapes of $F\exp1$ and $F\exp2$ also vary. Moreover, the crossover point has not been taken into account in the definitions of $Fih1$ and $Fih2$, thus risking a strong χ-dependence on shapes and x-positions of $F\exp1$ and $F\exp2$.

2. Significant deviation parameters derived from Weibull master curves

A highly appropriate evaluation method, which considers variations in shape and position of the deviation areas, will be presented in this section. It can be applied to all three types of Weibull master curves, i.e., $I(x, m)$, $K(y, m)$, and $M[e(z), m]$ as defined in part 1 [1]. It will be developed for $M[e(z), m]$, as being the general type of master curve containing $I(x, m)$ and $K(y, m)$ as special cases. First, another step function $H[e(z)]$ equal to zero for scaled failure stresses $e(z) < e_{cr}(z)$ and equal to one for $e(z) \geq e_{cr}(z)$, is defined. $e_{cr}(z)$ represents the value corresponding to the cross-over point formed by $M[e(z), m]$ and the experimental Weibull master curve $M\exp[e(z), m]$. The step function $H[e(z)]$ represent materials, which fail at $e(z) = e_{cr}(z)$ in a deterministic way, i.e., the fracture processes leading to failure are fully controlled by the toughening mechanisms responsible for stable crack growth. Thus, the scaled failure stress distributions of such materials are independent of the initial defect-size distributions [2, 3, 9]. The two areas formed between the step function $H[e(z)]$ and $M[e(z), m]$ are denoted by $FiM1[e(z)]$ and $FiM2[e(z)]$. In addition, $I(x, m)$ is equivalent to $M[e(z_{in}), m]$, whereby z_{in} is defined by

$$z_{in} = P(\sigma_{in}) = 1 - \exp\left(\frac{1-m}{m}\right) \tag{2}$$

$$\sigma(z_{in}) = \sigma_{in} \tag{3}$$

$$e(z_{in}) = \frac{\sigma - \sigma_\tau}{\sigma_{in} - \sigma_\tau} = x \tag{4}$$

Furthermore, $K(y, m)$ is equivalent to $M[e(\overline{z}), m]$ representing the other special case of $M[e(z), m]$, which

fulfills the condition $FiM1[e(z)] - FiM2[e(z)] = 0$, if $e_{cr}(z)$ is equal to one. $\bar{z}$ is defined as follows:

$$\bar{z} = P(\bar{\sigma}) = 1 - \exp\left\{-\left[\Gamma\left(1+\frac{1}{m}\right)\right]^m\right\} \quad (5)$$

$$\bar{\sigma} = \sigma(\bar{z}) = \int_0^1 \sigma \, dP = \sigma_\tau + \sigma_0 \Gamma\left(1+\frac{1}{m}\right) \quad (6)$$

$$e(\bar{z}) = \frac{\sigma - \sigma_\tau}{\bar{\sigma} - \sigma_\tau} = y \quad (7)$$

$F\exp1M[e(z)]$ and $F\exp2M[e(z)]$ represent the two areas formed between $M\exp[e(z), m]$ and $M[e(z), m]$, whereby $M\exp[e(z), m]$ is constructed by calculating the Weibull modulus m from the upper σ-range of experimental, cumulative failure stress probability distribution $P(\sigma_i)$. The following equations result from the application of the evaluation method developed in reference [2]:

$$FiM1[e(z)] = \int_0^{e_{cr}(z)} M[e(z), m]\, d[e(z)] = \int_0^{e_{cr}(z)} \left\{1 - (1-z)^{[e(z)]^m}\right\} d[e(z)] \quad (8)$$

$$FiM2[e(z)] = \int_{e_{cr}(z)}^{\infty} \{1 - M[e(z), m]\}\, d[e(z)] = \int_{e_{cr}(z)}^{\infty} \left\{(1-z)^{[e(z)]^m}\right\} d[e(z)] \quad (9)$$

$$F\exp1M[e(z)] = \int_0^{e_{cr}(z)} |M\exp[e(z), m] - M[e(z), m]|\, d[e(z)] \quad (10)$$

$$F\exp2M[e(z)] = \int_{e_{cr}(z)}^{\infty} |M[e(z), m] - M\exp[e(z), m]|\, d[e(z)] \quad (11)$$

Between $FiM1[e(z)]$ and $FiM2[e(z)]$ the following relation is valid:

$$FiM1[e(z)] - FiM2[e(z)] = e_{cr}(z) - \int_0^{\infty} \exp\{[ln(1-z)][e(z)]^m\}\, d[e(z)] = e_{cr}(z) - \frac{\Gamma\left(1+\frac{1}{m}\right)}{[-ln(1-z)]^{\frac{1}{m}}} \quad (12)$$

whereby Equations 8 and 9 as well as the following identities are used:

$$(1-z)^{[e(z)]^m} = \exp\left\{ln\left[(1-z)^{[e(z)]^m}\right]\right\} = \exp\{[e(z)]^m ln(1-z)\} \quad (13)$$

The specimen-size-independent, material-specific quotient χ_M is then given by

$$\chi_M = \left\{\frac{FiM1[e(z)]}{FiM2[e(z)]}\right\} : \left\{\frac{F\exp1M[e(z)]}{F\exp2M[e(z)]}\right\} \quad (14)$$

The χ_M-values of the special master curves $I(x, m)$ and $K(y, m)$, denoted by χ_I and χ_k, are obtained by replacing z with z_{in} or $\bar{z}$ in equations (8–14):

$$\chi_I = \left\{\frac{FiM1[e(z_{in})]}{FiM2[e(z_{in})]}\right\} : \left\{\frac{F\exp1M[e(z_{in})]}{F\exp2M[e(z_{in})]}\right\} \quad (15)$$

$$\chi_k = \left\{\frac{FiM1[e(\bar{z})]}{FiM2[e(\bar{z})]}\right\} : \left\{\frac{F\exp1M[e(\bar{z})]}{F\exp2M[e(\bar{z})]}\right\} \quad (16)$$

The quotients χ_M, χ_I, and χ_k are material-specific in a first approach, as has already been shown for χ by Lambrigger [2]. However, all these quotients remain m-dependent, thus complicating comparisons between materials with highly different Weibull moduli m. At least calibration has been made easier because shapes and positions of the areas $F\exp1M$ and $F\exp2M$, being separated by the cross-over point, are considered by integration up to $e_{cr}(z)$ in all the relevant equations (8–11). The latter is not the case for the quotient χ defined by Equation 1 and as suggested in an earlier paper [2].

3. Significant deviation parameters derived from apparent fracture toughness master curves

The theoretical, apparent fracture toughness master curves $L[d(z)]$ have already been discussed in detail in part 1 [1]. However, an additional step function through the inflexion point of $L[d(z)]$, which is equal to zero for the scaled failure stress intensities $d(z) < d_{cr}(z)$ and equal to one for $d(z) \geq d_{cr}(z)$, can be defined representing formally a material undergoing 0% unstable crack extension. Furthermore, $d_{cr}(z)$ represents the value of the cross-over point formed by $L[d(z)]$ and $L\exp[d(z)]$. Between this step function and $L[d(x)]$, two areas are formed, $C_{1\infty}$ below and $C_{2\infty}$ above the cross-over of the two curves at $d(z) = 1$. The values of $C_{1\infty}$ and $C_{2\infty}$ thus correspond to 0% unstable crack extension. The values of the areas formed between $L[d(z)]$ and $L\exp[d(z)]$ generally represent fracture events with a limited percentage of stable crack extension. They are denoted by $C1\exp$ and $C2\exp$, if two such areas are formed. $C1\exp$ represents in these cases the area below, and $C2\exp$ represents the area above the cross-over $d_{cr}(z)$ formed by $L\exp[d(z)]$ and $L[d(z)]$. $C_{1\infty}$, $C1\exp$, $C_{2\infty}$, and $C2\exp$ are calculated as follows:

$$C_{1\infty} = \int_0^{d_{cr}(z)} L[d(z)]\, d[d(z)] = \int_0^{e_{cr}(z)} \left(1 - \exp\left\{[-ln(1-z)]^{\frac{m-4}{4}} \times [-ln(1 - M[e(z), m])]^{\frac{4}{m}}\right\}\right) d[e(z)] \quad (17)$$

$$C_{2\infty} = \int_{d_{cr}(z)}^{\infty} \{1 - L[d(z)]\}\, d[d(z)] = \int_{e_{cr}(z)}^{\infty} \left(\exp\left\{[-ln(1-z)]^{\frac{m-4}{4}} \times [-ln(1 - M[e(z), m])]^{\frac{4}{m}}\right\}\right) d[e(z)] \quad (18)$$

$$|C_{1\infty} - C1\exp| = \int_0^{d_{cr}(z)} L\exp[d(z)]\, d[d(z)]$$
$$= \int_0^{e_{cr}(z)} \left(1 - \exp\left\{[-ln(1-z)]^{\frac{m-4}{4}} \times [-ln(1 - M\exp[e(z), m])]^{\frac{4}{m}}\right\}\right) \times d[e(z)] \quad (19)$$

$$|C_{2\infty} - C2\exp| = \int_{d_{cr}(z)}^{\infty} \{1 - L\exp[d(z)]\}\, d[d(z)]$$
$$= \int_{e_{cr}(z)}^{\infty} \left(\exp\left\{[-ln(1-z)]^{\frac{m-4}{4}} \times [-ln(1 - M\exp[e(z), m])]^{\frac{4}{m}}\right\}\right) \times d[e(z)] \quad (20)$$

The corresponding expressions for the special master curves $I(x, m)$ or $K(y, m)$ are obtained, by replacing $L[d(z)]$ through $N(a) = L[d(z_{in})]$ or $T(b) = L[d(\overline{z})]$, as well as $M[e(z), m]$ through $I(x, m) = M[e(z_{in}), m]$ or $K(y, m) = M[e(\overline{z}), m]$ in Equations 17 and 18. Moreover, the analogous replacements have to be carried out with the experimental master curves $L\exp[d(z)]$ and $M\exp[e(z), m]$ in Equations 19 and 20. As in the case of Weibull master curves, a material-specific quotient χ_B can also be defined for apparent fracture toughness master curves in the following manner:

$$\chi_B = \left(\frac{C_{1\infty}}{C_{2\infty}}\right) : \left(\frac{C1\exp}{C2\exp}\right) \quad (21)$$

The deviation parameters derived from apparent fracture toughness master curves are m-independent, fascilitating direct comparisons of completely different types of materials. They can be interpreted with the help of the two component models of Cook and Clarke [3]. This interpretation is also possible for the deviation parameters derived from Weibull master curves, however, calibration problems can arise.

4. Model of Cook and Clarke

The areas $C1\exp$ and $C2\exp$ can be interpreted with the help of the two-component model described by Cook and Clarke [3]. Cook and Clarke modelled the driving force for fracture as the sum of two components, one stabilizing and the other destabilizing crack propagation, leading to a crack extension force displaying a minimum as a function of crack length. The resistance to crack extension, the R-curve, is described in this two-component model by an increasing power law $R \propto c^{2\tau}$ (c being the crack length, R the fracture resistance, and τ the toughening exponent, characterizing the rate of toughness increase) overlapped by an additional, localized loading, decreasing the driving force for fracture with increasing crack length. The localized loading is modelled by a residual stress intensity factor. Using equilibrium fracture criteria, it is thus possible to describe the fracture behavior of brittle materials, which undergo an amount of stable crack growth before failure occurs by unstable crack extension. If the two-component model of Cook and Clarke is used to interprete the areas $C1\exp$ and $C2\exp$, it can be observed that, within the framework of this approach, values, shapes, and positions of $C1\exp$ and $C2\exp$ are only dependent on the toughening exponent τ describing the rising R-curve behavior, and on the type, localization, and number of residual stress fields existing in the investigated specimens. Because the toughening exponent τ is generally valid in the whole specimen, it is a characteristic value of the material. The localized component of the stress intensity factor is attributed to defects producing the residual stress fields in the specimen. It is supposed that the residual stress fields mainly determine the shape, value, and position relative to the $d(z)$-axis of $C2\exp$ (i.e., also the $d_{cr}(z)$-value), the toughening exponent, τ, however, predominantly the value of $C1\exp$. The type, degree of localization, and number of residual stress fields in the material and, therefore, $d_{cr}(z)$ and $C2\exp$, are thus believed to determine, in a first approach, the toughening behavior of brittle materials with respect to the stable growth of microracks, if an external load is applied; for the growth of microcracks is controlled by microstructural features, and finally results in local stress release. The toughening exponent, τ, on the other hand, is thought to determine predominantly the toughening behavior based on the increased fracture resistance in the lower $d(z)$-range of large cracks, mainly due to crack-tip shielding. The crack growth of large cracks is principally controlled by the continuum properties of the material.

Because in quasi-static uniaxial bend tests, a compression region is formed in the tested specimens, which is the sum of localized residual stress fields decreasing the driving force for fraction, it is thought that experimental, apparent fracture toughness master curves $L\exp[d(z)]$, obtained from quasi-static uniaxial bend tests, might slightly differ from those of uniaxial tensile tests, if very large stable crack growth of relatively small cracks takes place prior to failure. In uniaxial tensile tests, no additional residual stress fields of this type, decreasing the driving force for fraction, are created. Therefore, the $C1\exp$- and specially the $C2\exp$-values obtained from uniaxial bend tests might be overestimated in these cases. The values of $C1\exp$ and $C2\exp$ might also turn out to be slightly specimen-size-dependent in uniaxial tensile tests if the residual stresses built up in the tested specimens are both extremely high and clearly not proportional to the applied stress, because in these cases, the Weibull modulus m is not necessarily specimen-size-independent, according to Weibull [4, 5].

5. Experimental data of three-point bend tests

The experimental Weibull master curve $K\exp(y, m = 7.9)$ and the corresponding experimental, apparent fracture toughness master curve $T\exp(b)$ of 12 mol % ceria partially stabilized tetragonal zirconia polycrystals (Ce-TZP) are displayed in Figs 1 and 2. These

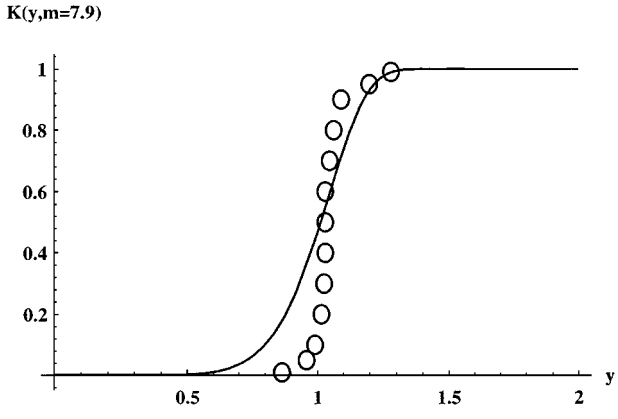

Figure 1 Dashed line: Experimental, alternative Weibull master curve $K\exp(y, m = 7.9)$ of Ce-TZP calculated from three-point bend tests of Ready and McCallen [6]. Full line: Alternative Weibull master curve $K(y, m = 7.9)$.

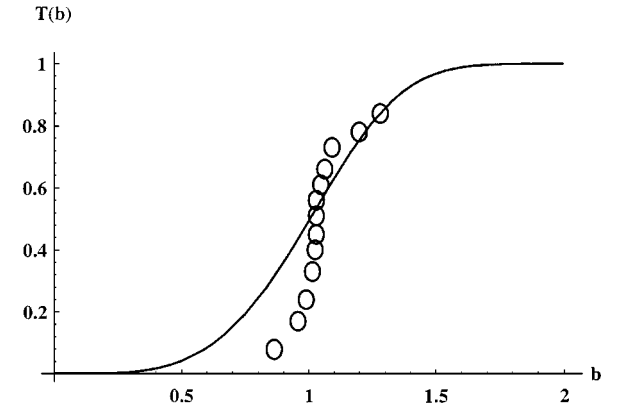

Figure 2 Dashed line: Experimental, alternative apparent fracture toughness master curve $T\exp(b)$ of Ce-TZP calculated from $K\exp(y, m = 7.9)$. Full line: Alternative master curve for brittle cleavage fracture toughness testing $T(b)$.

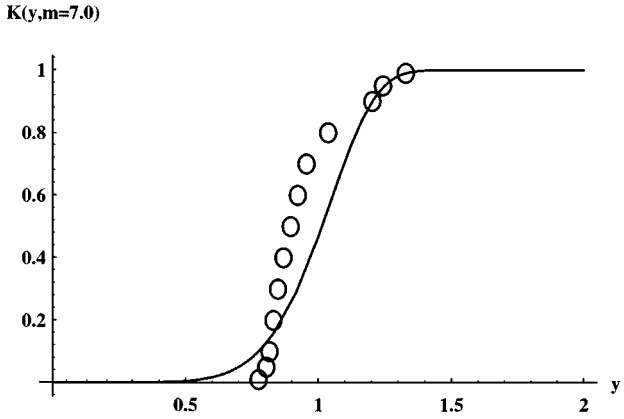

Figure 3 Dashed line: Experimental, alternative Weibull master curve $K\exp(y, m = 7.0)$ of Y-PSZ/β-alumina composite calculated from three-point bend tests of Troczynski and Nicholson [7]. Full line: Alternative Weibull master curve $K(y, m = 7.0)$.

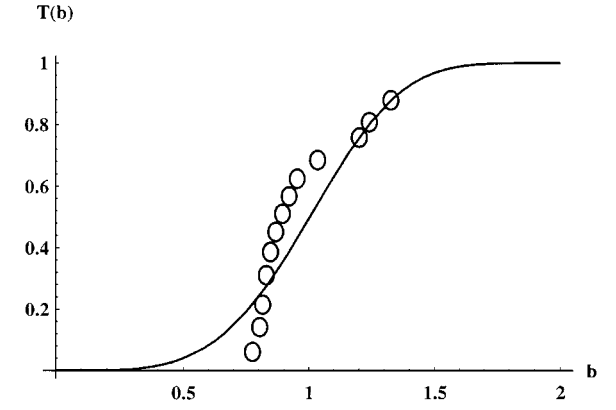

Figure 4 Dashed line: Experimental, alternative apparent fracture toughness master curve $T\exp(b)$ of Y-PSZ/β-alumina composite calculated from $K\exp(y, m = 7.0)$. Full line: Alternative master curve for brittle cleavage fracture toughness testing T(b).

master curves have been derived from quasi-static three-point bend tests of Ready and McCallen [6] performed at room temperature. The master curves $K(y, m)$ and $T(b)$ are most convenient for describing quasi-static, mechanical tests characterized by uniaxial stress distributions because the mean, representing the physically highly significant first moment, is used as scaling factor and, moreover, $K(y, m)$ exists for every relevant Weibull modulus $m > 0$. The following characteristic deviation parameters have been evaluated for Ce-TZP: $m \approx 7.9$, $y_{cr} \approx 1.03$, $b_{cr} \approx 1.03$, $\chi_k \approx 0.22$, $\chi_B \approx 0.18$, $(\chi_k/\chi_B) \approx 1.26$, $FiM1[e(\bar{z})] \approx 0.075$, $FiM2[e(\bar{z})] \approx 0.098$, $F\exp1M[e(\bar{z})] \approx 0.062$, $F\exp2M[e(\bar{z})] \approx 0.018$, $C_{1\infty} \approx 0.1285$, $C_{2\infty} \approx 0.0985$, $(C1\exp/C_{1\infty}) \approx 69\%$, and $(C2\exp/C_{2\infty}) \approx 12\%$.

The experimental Weibull master curve $K\exp(y, m = 7.0)$ and the experimental, apparent fracture toughness master curve $T\exp(b)$ of 8 wt % yttria partially stabilized zirconia/20 vol % β-alumina composite (Y-PSZ/β-alumina composite) are displayed in Figs 3 and 4. These master curves have been derived from quasi-static three-point bend tests performed at room temperature by Troczynski and Nicholson [7]. The following characteristic deviation parameters have been evaluated for Y-PSZ/β-alumina composite: $m \approx 7.0$, $y_{cr} \approx 0.83$, $b_{cr} \approx 0.82$, $\chi_k \approx 0.40$, $\chi_B \approx 0.24$, $(\chi_k/\chi_B) \approx 1.67$, $FiM1[e(\bar{z})] \approx 0.017$, $FiM2[e(\bar{z})] \approx 0.187$, $F\exp1M[e(\bar{z})] \approx 0.014$, $F\exp2M\ [e(\bar{z})] \approx 0.062$, $C_{1\infty} \approx 0.0461$, $C_{2\infty} \approx 0.2260$, $(C1\exp/C_{1\infty}) \approx 82\%$ and $(C2\exp/C_{2\infty}) \approx 19\%$. It is obvious, that the Weibull moduli m of Ce-TZP and Y-PSZ/β-alumina differ only slightly. However, the shapes and positions of the deviation areas $F\exp1M[e(\bar{z})]$, $F\exp2M[e(\bar{z})]$, $C1\exp$ and $C2\exp$ are completely different. The latter leads to quite different cross-over values y_{cr} and b_{cr}, characterizing in a first approach shapes and positions of the deviation areas. Furthermore, the (χ_k/χ_B)-values of the two materials are close to one another. Therefore, because χ_B is an m-independent magnitude, it can be concluded also that deviation parameters of Weibull master curves of different types of materials might be compared to one another, as long as the values of the Weibull moduli m do not differ significantly. Further, the deviation areas have to be defined in the suggested way by taking account of the cross-over values in the form of integration limits.

The experimental Weibull master curve $K\exp(y, m = 25)$ and $T\exp(b)$ of a coarse-grained β-silicon nitride are displayed in Figs 5 and 6. These master curves

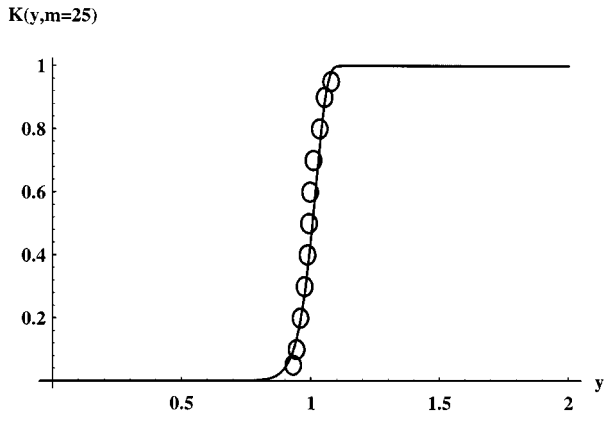

Figure 5 Dashed line: Experimental, alternative Weibull master curve $K\exp(y, m = 25)$ of coarse-grained β-silicon nitride calculated from three-point bend tests of Hirosaki and Akimune [8]. Full line: Alternative Weibull master curve $K(y, m = 25)$.

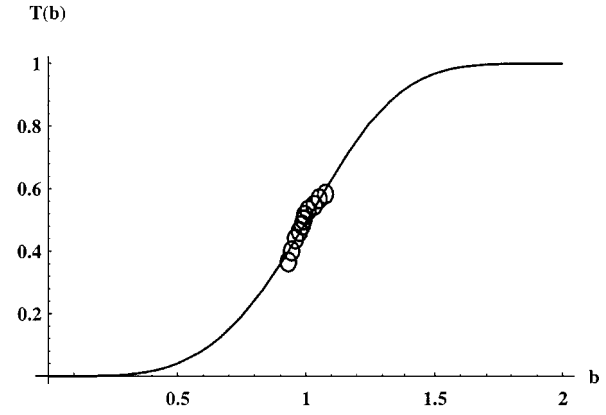

Figure 6 Dashed line: Experimental, alternative apparent fracture toughness master curve $T\exp(b)$ of coarse-grained β-silicon nitride calculated from $K\exp(y, m = 25)$. Full line: Alternative master curve for brittle cleavage fracture toughness testing $T(b)$.

are again derived from quasi-static three-point bend tests being performed at room-temperature by Hirosaki and Akimune [8]. It can be seen from Fig. 6 that $C1\exp$ cannot be evaluated graphically from $T\exp(b)$ for statistical reasons. According to Equation 24 of part 1 [1], it can be seen that the high value of the Weibull modulus m reduces $T\exp(b)$ to a very narrow b-range close to 1 for measurements based on about twenty tested specimens. Nevertheless, $K\exp(y, m = 25)$ facilitates an acceptable fit down to $y = 0$. Thus, at least $F\exp1M[e(\overline{z})]$ can be evaluated directly. Morevoer, $C1\exp$ can be obtained analytically by simply using Equation 19 in the special case of $K\exp(y, m)$.

$$
\begin{aligned}
|C_{1\infty} - C1\exp| &= \int_0^{b_{cr}} T\exp(b)\,db \\
&= \int_0^{y_{cr}} \left(1 - \exp\left\{-\Gamma\left(1+\frac{1}{4}\right)^4 \right.\right. \\
&\quad \times \left\{-\Gamma\left(1+\frac{1}{m}\right)^{-m} \right. \\
&\quad \left.\left.\left. \times ln[1 - K\exp(y, m)]\right\}^{\frac{4}{m}}\right\}\right) dy
\end{aligned}
\tag{22}
$$

The following characteristic deviation parameters have thus been evaluated for coarse-grained β-silicon nitride: $m \approx 25.0$, $y_{cr} \approx 0.98$, $b_{cr} \approx 0.98$, $\chi_k \approx 0.32$, $\chi_B \approx 0.08$, $(\chi_k/\chi_B) \approx 3.8$, $FiM1[e(\overline{z})] \approx 0.012$, $FiM2[e(\overline{z})] \approx 0.032$, $F\exp1M[e(\overline{z})] \approx 0.005$, $F\exp2M[e(\overline{z})] \approx 0.004$, $C_{1\infty} \approx 0.1036$, $C_{2\infty} \approx 0.1236$, $(C1\exp/C_{1\infty}) \approx 24\%$, and $(C2\exp/C_{2\infty}) \approx 2\%$. Although shapes and positions of the areas described by the deviation magnitudes $F\exp1M[e(\overline{z})]$, $F\exp2M[e(\overline{z})]$, $C1\exp$, $C2\exp$, y_{cr} and b_{cr} are quite similar to the ones evaluated for Ce-TZP, a clearly differnt quotient (χ_k/χ_B) has been discovered for the two materials. Therefore (χ_k/χ_B) is a considerably varying function with respect to the Weibull modulus m. Consequently, if it is intended to compare directly the deviation magnitudes of Weibull master curves of materials with completely different m-values, a calibration function $\frac{\chi_k}{\chi_B}(m)$ has to be available.

6. Discussion

In agreement with the model of Cook and Clarke [3], a high $(C1\exp/C_{1\infty})$-value can be explained as an efficient shielding of the crack-tips of large cracks. This is clearly the case for Ce-TZP and Y-PSZ/β-alumina composite. On the other side, a high $(C2\exp/C_{2\infty})$-value combined with $d_{cr}(z) \approx 1$ indicates a huge amount of simultaneous, stable growth of microcracks as well as a narrow initial defect-size distribution. If the initial defect-size distribution had not been narrow, $d_{cr}(z)$ would have been decreased clearly below 1 by the growing defects belonging to the large-size tail of the initial defect-size distribution. For Ce-TZP, all of the mentioned conditions are fulfilled, whereas for β-silicon nitride only a narrow initial defect-size distribution as well as a moderate shielding of large cracks might be supposed. Furthermore, the initial defects represent the potential starting points for microcracking (i.e., the nucleation sites of the microcracks).

In the case of Y-PSZ/β-alumina composite, quite high $(C1\exp/C_{1\infty})$- and $(C2\exp/C_{2\infty})$-values have been evaluated indicating efficient shielding of crack-tips of large cracks as well as intense stable microcracking. However, $d_{cr}(z)$ is clearly smaller than 1, thus giving rise to the assumption of a wide initial defect-size distribution as well as simultaneous, intense stable growth of microcracks of a wide size-range prior to failure. This situation can characteristically be expected, if debonding occurs along inhomogenities, such as grain-boundaries and internal interfaces, and is characterized by local, detrimental defect-size distributions as well as high, local concentrations of defects. For example, in the case of the Y-PSZ/β-alumina composite, significant debonding along the interfaces of the two phases has been claimed [9].

It is assumed that the positions of $C1\exp$ and $C2\exp$ relative to the $d(z)$-axis, as well as the values and shapes of these two areas, might provide additional information about the toughening mechanisms operating in macroscopically homogeneous materials undergoing stable crack growth, if experimental data of materials of known toughening mechanisms are available

as calibration curves. In addition, typical toughening mechanisms are crack-branching, crack-deflection, stable growth of microcraks, network-formation of microcracks, and ductile tearing. (Also, combinations of several mechanisms might not be rare.) The toughening mechanisms are mainly relevant in crack-tip shielding of larger cracks, stable growth of (micro-) cracks as well as (micro-) crack nucleation from initial defects.

Furthermore, the whole discussion could also have been performed merely on the basis of Weibull master curves $M[e(z), m]$ and on the corresponding deviation parameters χ_M, $e_{cr}(z)$, $F\exp 1M$ and $F\exp 2M$; however, direct interpretation would be nearly impossible, as long as calibration curves are not available, and as long as it is not clear up to what degree χ_M is shape- and $e_{cr}(z)$-independent.

References

1. M. LAMBRIGGER, submitted to *J. Mater. Sci.*
2. *Idem, J. Mater. Sci. Lett.* **16** (1997) 924.
3. R. F. COOK and D. R. CLARKE, *Acta Metall.* **36** (1988) 555.
4. W. WEIBULL, Ingeniörvetenskapakademien, Handlingar No. 151, Stockholm (1939).
5. *Idem, ibid.*, Handlingar No. 153, Stockholm (1939).
6. M. J. READY and C. I. MCCALLEN, *J. Am. Ceram. Soc.* **78** (1995) 2769.
7. T. B. TROCZYNSKI and P. S. NICHOLSON, *ibid.* **68** (1985) C-277.
8. K. HIROSAKI and Y. AKIMUNE, *ibid.* **76** (1993) 1892.
9. M. LAMBRIGGER, *Phil. Mag. A* **77** (1998) 363.

Received 29 July
and accepted 26 August 1998